

## Cross-phase-modulation-induced instability in photonic-crystal fibers

E. E. Serebryannikov,<sup>1</sup> S. O. Konorov,<sup>1</sup> A. A. Ivanov,<sup>3</sup> M. V. Alfimov,<sup>3</sup> M. Scalora,<sup>4</sup> and A. M. Zheltikov<sup>1,2,\*</sup>

<sup>1</sup>*Physics Department, M.V. Lomonosov Moscow State University, 119899 Moscow, Russia*

<sup>2</sup>*International Laser Center, M.V. Lomonosov Moscow State University, 119899 Moscow, Russia*

<sup>3</sup>*Center of Photochemistry, Russian Academy of Sciences, Novatorov 7a, Moscow 117421, Russia*

<sup>4</sup>*Charles M. Bowden Research Center, Weapons Sciences Directorate, US Army Aviation and Missile Command, Huntsville, Alabama 35898-5000, USA*

(Received 4 April 2005; published 31 August 2005)

Cross-phase-modulation-induced instability is identified as a significant mechanism for efficient parametric four-wave-mixing frequency conversion in photonic-crystal fibers. Fundamental-wavelength femtosecond pulses of a Cr: forsterite laser are used in our experiments to transform the spectrum of copropagating second-harmonic pulses of the same laser in a photonic-crystal fiber. Efficient generation of sidebands shifted by more than 80 THz with respect to the central frequency of the second harmonic is observed in the output spectrum of the probe field.

DOI: 10.1103/PhysRevE.72.027601

PACS number(s): 42.65.Wi

Photonic-crystal fibers (PCFs) [1] offer attractive strategies for the enhancement of nonlinear-optical processes. In addition to the standard recipes of nonlinear optics of guided waves, viz., large interaction lengths and phase matching achieved through a balance between material and waveguide dispersion components [2], PCFs suggest important benefits related to their unique properties. High refractive index steps attainable with a PCF design can strongly confine the light field in the fiber core, adding quite substantially to the enhancement of nonlinear-optical phenomena [3,4]. Perhaps, even more important is that the dispersion of guided modes in PCFs can be tailored by modifying the PCF structure [5], offering phase- and group-index-matching solutions and allowing the wavelength of zero group-velocity dispersion (GVD) to be tuned within a broad spectral range. The tunability of the zero-GVD point leads to solitonic regimes, allowing the frequency of ultrashort laser pulses to be efficiently down-converted through soliton self-frequency shift [6] and up-converted through the Cherenkov emission of dispersive waves [7]. As a result, the enhancement of a whole catalog of nonlinear-optical phenomena has been demonstrated with PCFs, with efficient frequency conversion and spectral transformation implemented through soliton frequency shifts [6] and dispersive-wave emission [7], four-wave mixing (FWM) [8], stimulated Raman scattering [9], and third-harmonic generation [10–12].

In this work, modulation instability (MI) induced by cross-phase modulation (XPM) [2] is identified as an important mechanism of frequency conversion in PCFs. Earlier experiments have demonstrated that XPM can have a significant influence on supercontinuum generation [13] and anti-Stokes emission [14] in PCFs. Self-induced MI in PCFs, on the other hand, has been shown [15] to provide a convenient means for broadband parametric amplification, permitting the creation of compact and convenient all-fiber-optical parametric oscillators. We will show in this paper that

XPM-induced MI, which does not require anomalous dispersion [2,16], suggests convenient and practical control knobs for the frequency conversion of ultrashort pulses, allowing the frequency shifts and amplitudes of sidebands in output spectra of the probe field to be tuned by varying the amplitude of the pump field.

Photonic-crystal fibers used in our experiments were fabricated of fused silica using a standard technology, described in detail elsewhere [1]. The cross-section view of the PCF is shown in the inset to Fig. 1. The fiber core diameter was equal to 4.3  $\mu\text{m}$ . Figure 1 displays the group velocity and GVD calculated for this PCF using the polynomial-expansion technique [17]. The standard theory of XPM-induced MI, as presented by Agrawal [16], was used to analyze the main features of this phenomenon for fundamental-wavelength and second-harmonic femtosecond pulses of a Cr: forsterite laser copropagating in a PCF with the above-specified structure. This theory predicts that stationary solutions to slowly varying envelope approximation equations for the pump and probe fields including dispersion up to the second order become unstable with respect to a small harmonic perturbation with the wave vector  $K$  and the frequency

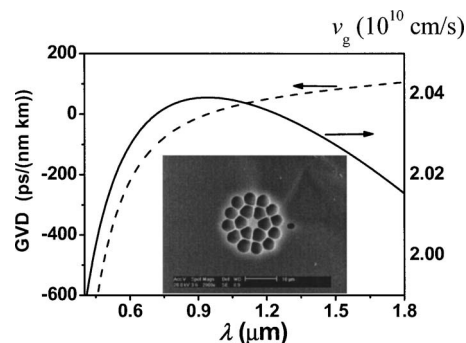


FIG. 1. The group velocity (the solid curve and the right-hand axis) and the group-velocity dispersion (the dashed curve and the left-hand axis) calculated as functions of the radiation wavelength  $\lambda$  for the fundamental mode of the PCF with a cross-section structure shown in the inset.

\*Electronic address: zheltikov@phys.msu.ru

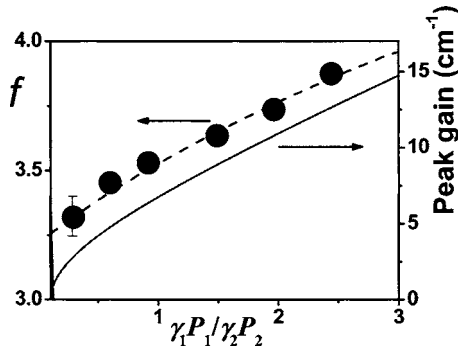


FIG. 2. The dimensionless frequency shift of the probe field  $f$  (the dashed line and left-hand axis) and the MI gain  $G$  (the solid line and the right-hand axis) calculated as functions of the ratio  $\gamma_1 P_1 / \gamma_2 P_2$ . The filled circles represent the experimentally measured frequency shifts of the short-wavelength sideband in the spectrum of the probe field.

$\Omega$  if  $K$  has a nonzero imaginary part. The domains of this instability can be found by analyzing the dispersion relation  $[(K - \Omega \delta / 2)^2 - h_1][(K + \Omega \delta / 2)^2 - h_2] = C^2$ , where  $h_j = \beta_{2j}^2 \Omega^2 (\Omega^2 + 4 \gamma_j P_j / \beta_{2j}) / 4$ ,  $C = 2 \Omega^2 \sqrt{\beta_{21} \beta_{22} \gamma_1 \gamma_2 P_1 P_2}$ ,  $\gamma_j = n_2 \omega_j / (c S_j)$  are the nonlinear coefficients,  $\delta = (v_{g2})^{-1} - (v_{g1})^{-1}$ ,  $\beta_{2j} = (d^2 \beta_j / d\omega^2)_{\omega=\omega_j}$ ,  $P_j$ ,  $\omega_j$ ,  $v_{gj}$ , and  $\beta_j$  are the peak powers, the central frequencies, the group velocities, and the propagation constants of the pump ( $j=1$ ) and probe ( $j=2$ ) fields,  $n_2$  is the nonlinear refractive index, and  $S_j$  are the effective mode areas for the pump and probe fields. The gain of instabilities with a wave number  $K$  is given by  $G(\Omega) = 2 \text{Im}(K)$ .

Analysis of dispersion properties for the PCFs employed in our experiments (Fig. 1) yields  $\beta_{21} \approx -500 \text{ fs}^2/\text{cm}$ ,  $\beta_{22} \approx 400 \text{ fs}^2/\text{cm}$ , and  $\delta = 150 \text{ fs}/\text{cm}$ . In Fig. 2, we plot the dimensionless frequency shift of the probe field,  $f = \Omega / \Omega_c$  [where  $\Omega_c = (4 \gamma_2 P_2 / |\beta_{22}|)^{1/2}$ ] and the gain  $G$  calculated as functions of the ratio  $\gamma_1 P_1 / \gamma_2 P_2$ . The frequency shift  $f$  changes from approximately 3.3 up to 3.8 as the  $\gamma_1 P_1 / \gamma_2 P_2$  ratio is varied from 0.3 to 2.5. As highlighted by Agrawal [16], such a weak dependence of the frequency shift of the probe field on the pump power is typical of XPM-induced MI in the regime of pump-probe group-velocity mismatch. With  $\gamma_2 P_2 \approx 1.5 \text{ cm}^{-1}$ , the frequency shift  $f \approx 3.8$  gives sidebands shifted by  $\Omega / 2\pi \approx 74 \text{ THz}$  with respect to the central frequency  $\omega_2$  of the second harmonic (which corresponds to approximately 90 nm on the wavelength scale). As will be shown below, this prediction agrees well with our experimental results.

The laser system used in our experiments consisted of a  $\text{Cr}^{4+}$ : forsterite master oscillator, a stretcher, an optical isolator, a regenerative amplifier, and a compressor. The master oscillator, pumped with a fiber ytterbium laser, generated 30 – 60 fs light pulses of radiation with a wavelength of 1.23–1.25  $\mu\text{m}$  at a repetition rate of 120 MHz. These pulses were then transmitted through a stretcher and an isolator, to be amplified in a Nd: YLF-laser-pumped amplifier and recompressed to the 170 fs pulse duration with the maximum laser pulse energy up to 40  $\mu\text{J}$  at 1 kHz. A 1 mm thick BBO crystal was used to generate the second harmonic of ampli-

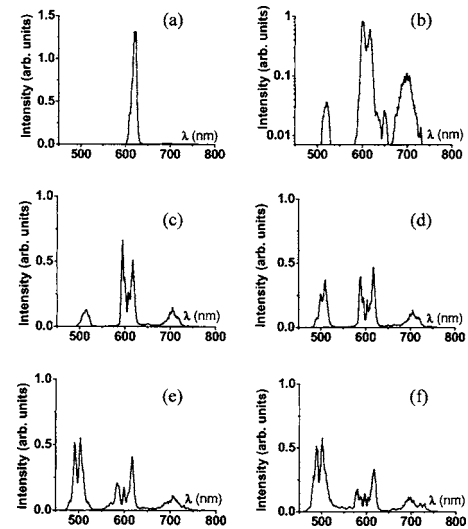


FIG. 3. Output spectra of the second-harmonic field transmitted through a 5 cm PCF. The power of the pump pulses is (a) 3, (b) 7, (c) 30, (d) 42, (e) 70, and (f) 100 kW. The power of the probe pulse is 8 kW.

fied Cr: forsterite laser radiation. Fundamental wavelength, 1235 nm radiation of a femtosecond Cr: forsterite laser and its second harmonic were used as pump and probe fields, respectively. As can be seen from Fig. 1, the pump wavelength in our experiments falls within the area of anomalous dispersion for the fundamental mode of the PCF, while the second-harmonic probe lies in the range of normal dispersion. The faster pump pulse (see Fig. 1) was delayed in our experiments with respect to the slower probe pulse at the input of the PCF by a variable delay time  $\tau$ .

Figures 2 and 3 present the results of experimental measurements performed with 170 fs pump pulses (fundamental radiation of the Cr: forsterite laser) with an energy ranging from 0.2 up to 20 nJ and 3 nJ 180 fs probe pulses (the second-harmonic output of the Cr: forsterite laser) transmitted through a 5 cm PCF with the cross-section structure shown in the inset to Fig. 1. For delay times  $\tau$  around zero, the slower probe pulse sees only the trailing edge of the faster moving pump pulse. In such a situation, XPM predominantly induces a blueshift of the probe field. For  $\tau \approx \delta L \approx 750 \text{ fs}$ , where  $L = 5 \text{ cm}$  is the PCF length, the leading edge of the pump pulse catches up with the probe field closer to the output end of the fiber, which results in a predominant redshift of the probe. To symmetrize the interaction between the pump and probe fields with respect to the XPM-induced frequency shift, we choose the delay time  $\tau = \delta L / 2 \approx 375 \text{ fs}$ . In the regime of low pump peak powers (less than 3 kW), the output spectrum of the probe field displays only slight broadening due to self-phase modulation [Fig. 3(a)]. Pump pulses with higher peak powers lead to radical changes in the output spectra of the probe field, splitting the central spectral component of the probe field and giving rise to intense symmetric sidebands around the central frequency  $\omega_2$  [Figs. 3(b)–3(d)].

The general tendencies in the behavior of the output spectrum of the probe field as a function of the pump power agree well with the prediction of the standard theory of

XPM-induced MI. In Fig. 2, we compare theoretical predictions for the dimensionless frequency shift of the probe field  $f$  calculated as a function of the ratio  $\gamma_1 P_1 / \gamma_2 P_2$  (the dashed line) with experimentally measured frequency shifts for the short-wavelength sideband in the spectrum of the probe field (filled circles). In view of the splitting and slight blueshifting of the central spectral component of the probe field [cf. Figs. 3(a)–3(d)], we define the effective central wavelength of the pump-broadened probe spectrum as 605 nm. As the pump power changes from 5 kW up to 42 kW in our experiments, the shift of the short-wavelength sideband in the output spectrum of the second harmonic increases from 80 nm up to approximately 90 nm. The theory predicts the wavelength shifts of 76 and 90 nm, respectively, indicating the predominant role of XPM-induced MI in the observed spectral transformations of the probe field. The amplitudes of sidebands generated by pump pulses with a peak power of about 40 kW, as can be seen from Fig. 3(d), become comparable or may even exceed the amplitude of the spectral components at the central part of the probe spectrum. The maximum frequency shift of probe-field sidebands achieved in our experiments with 45 kW pump pulses is estimated as 80 THz, which is substantially larger than typical frequency shifts resulting from XPM-induced MI in conventional fibers [2,18]. With pump powers higher than 50 kW, both the central spectral components of the probe field and its sidebands featured a considerable broadening [Figs. 3(e) and 3(f)] and tended to

merge together, apparently due to the cross-phase modulation induced by the pump field.

We have shown in this work that XPM-induced instabilities open an efficient channel of parametric FWM frequency conversion in photonic-crystal fibers. Fundamental-wavelength femtosecond pulses of a Cr: forsterite laser were used in our experiments as a pump field to generate intense sidebands around the central frequency of copropagating second-harmonic pulses of the same laser through XPM-induced MI in a PCF. This effect leads to efficient pump-field-controlled sideband generation in output spectra of the second-harmonic probe field.

The authors are grateful to Yu.N. Kondrat'ev, V.S. Shevandin, K.V. Dukel'skii, and A.V. Khokhlov for fabricating fiber samples. Illuminating discussions with M.V. Fedorov are gratefully acknowledged. This study was supported in part by the President of Russian Federation Grant No. MD-42.2003.02, the Russian Foundation for Basic Research (Contracts Nos. 03-02-16929, 04-02-81036-Bel2004, 04-02-39002-GFEN2004, and 03-02-20002-BNTS-a), and INTAS (Contracts Nos. 03-51-5037 and 03-51-5288). The research described in this publication was made possible in part by Grant No. RP2-2558 of the U.S. Civilian Research and Development Foundation for the Independent States of the Former Soviet Union (CRDF).

- 
- [1] P. St. J. Russell, *Science* **299**, 358 (2003).  
 [2] G. P. Agrawal, *Nonlinear Fiber Optics* (Academic, San Diego, 2001).  
 [3] M. A. Foster, K. D. Moll, and A. L. Gaeta, *Opt. Express* **12**, 2880 (2004).  
 [4] A. M. Zheltikov, *JETP* **97**, 505 (2003).  
 [5] W. H. Reeves, D. V. Skryabin, F. Biancalana, J. C. Knight, P. St. J. Russell, F. G. Omenetto, A. Efimov, and A. J. Taylor, *Nature (London)* **424**, 511 (2003).  
 [6] X. Liu, C. Xu, W. H. Knox, J. K. Chandalia, B. J. Eggleton, S. G. Kosinski, and R. S. Windeler, *Opt. Lett.* **26**, 358 (2001).  
 [7] J. Herrmann, U. Griebner, N. Zhavoronkov, A. Husakou, D. Nickel, J. C. Knight, W. J. Wadsworth, P. St. J. Russell, and G. Korn, *Phys. Rev. Lett.* **88**, 173901 (2002).  
 [8] J. M. Dudley, L. Provino, N. Grossard, H. Maillotte, R. S. Windeler, B. J. Eggleton, and S. Coen, *J. Opt. Soc. Am. B* **19**, 765 (2002).  
 [9] S. Coen, A. Hing Lun Chau, R. Leonhardt, J. D. Harvey, J. C. Knight, W. J. Wadsworth, and P. St. J. Russell, *J. Opt. Soc. Am. B* **19**, 753 (2002).  
 [10] J. K. Ranka, R. S. Windeler, and A. J. Stentz, *Opt. Lett.* **25**, 796 (2000).  
 [11] F. G. Omenetto, A. Taylor, M. D. Moores, J. C. Knight, P. St. J. Russell, and J. Arriaga, *Opt. Lett.* **26**, 1558 (2001).  
 [12] A. N. Naumov, A. B. Fedotov, A. M. Zheltikov, V. V. Yakovlev, L. A. Mel'nikov, V. I. Beloglazov, N. B. Skibina, and A. V. Shcherbakov, *J. Opt. Soc. Am. B* **19**, 2183 (2002).  
 [13] G. Genty, M. Lehtonen, and H. Ludvigsen, *Opt. Express* **12**, 4614 (2004).  
 [14] S. O. Konorov, A. A. Ivanov, D. A. Akimov, M. V. Alfimov, A. A. Podshivalov, Yu. N. Kondrat'ev, V. S. Shevandin, K. V. Dukel'skii, A. V. Khokhlov, M. Scalora, and A. M. Zheltikov, *New J. Phys.* **6**, 182 (2004).  
 [15] J. D. Harvey, R. Leonhardt, S. Coen, G. K. L. Wong, J. C. Knight, W. J. Wadsworth, and P. St. J. Russell, *Opt. Lett.* **28**, 2225 (2003).  
 [16] G. P. Agrawal, *Phys. Rev. Lett.* **59**, 880 (1987).  
 [17] T. M. Monro, D. J. Richardson, N. G. R. Broderick, and P. J. Bennet, *J. Lightwave Technol.* **18**, 50 (2000).  
 [18] J. E. Rothenberg, *Phys. Rev. A* **42**, R682 (1990).